Supplemental Document

applied optics

Power-balanced hybrid optics boosted design for achromatic extended depth-of-field imaging via optimized mixed OTF: supplement

SEYYED REZA MIRI ROSTAMI,* SAMUEL PINILLA, IGOR SHEVKUNOV, VLADIMIR KATKOVNIK, AND KAREN EGIAZARIAN

Computing Sciences Unit, Faculty of Information Technology and Communication Sciences, Tampere University, FI-33720 Tampere, Finland
*Corresponding author: *SeyyedReza.MiriRostami@tuni.fi**

Supplement DOI: https://doi.org/10.6084/m9.figshare.16663306

Parent Article DOI: https://doi.org/10.1364/AO.434852

Power-Balanced Hybrid Optics Boosted Design for Achromatic Extended-Depth-of-Field Imaging via Optimized Mixed OTF: Supplement

Seyyed Reza Miri Rostami[1,*], **Samuel Pinilla**[1], **Igor Shevkunov**[1], **Vladimir Katkovnik**[1], and **Karen Egiazarian**[1]

[1] *Computing Sciences Unit, Faculty of Information Technology and Communication Sciences, Tampere University, FI-33720 Tampere, Finland.*
[*] *Corresponding author: SeyyedReza.MiriRostami@tuni.fi*

Compiled September 21, 2021

This document provides supplementary information to the paper: 'Power-Balanced Hybrid Optics Boosted Design for Achromatic Extended-Depth-of-Field Imaging via Optimized Mixed OTF'. We present detailed analysis on the convergence behavior of the proposed design in the end-to-end optimization. We also provide the additional details about the physical experiments setup. The complementary experimental results are reported to show the advantage of the proposed image reconstruction algorithm and developed optical setup for achromatic extended depth of field (EDoF) imaging.

http://dx.doi.org/10.1364/ao.XX.XXXXXX

1. CONVERGENCE ANALYSIS OF DESIGN IN END-TO-END FRAMEWORK

This section is devoted to the numerical analysis of the convergence behavior of the loss function (Eq. (21) in the paper)

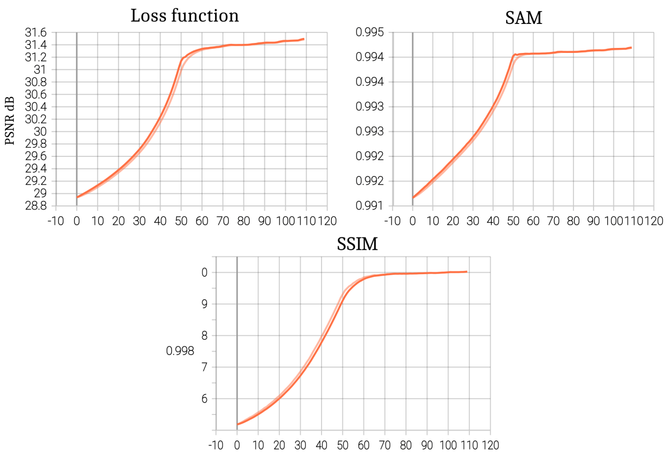

Fig. 1. The performance in terms of quality of the system design versus epochs is presented. These results are obtained when Fresnel order of MPM is equal to 1.4. Additional metrics such as Spectral Angular Mapper (SAM) and Structural Similarity Index (SSIM) are used for verification of the behavior of the design performance per epoch. These results prove that the proposed end-to-end design has a convergence behavior.

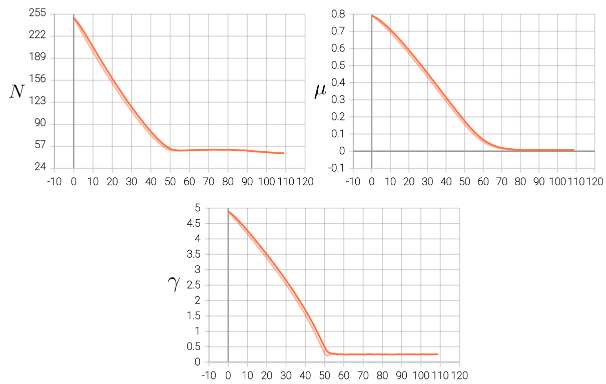

Fig. 2. Convergence behavior along epochs of the number of levels (N), variable μ of the designed mixed OTF, and Tikhonov regularization parameter γ are presented. These results are obtained when Fresnel order of MPM is equal to 1.4. These results prove that the optimizing variables either for inverse imaging and MPM of the proposed end-to-end design optic have a convergence behavior. In the case of the number of levels, the effectiveness of the smoothing approximation is verified.

along epochs in the proposed end-to-end design. Here, we report the resultant curves and additional verification quality imaging metrics such as Spectral Angular Mapper (SAM), and Structural Similarity Index (SSIM) using the TensorFlow library TensorBoard[1]. To make the end-to-end design differentiable, a smoothing function considered for designing the flat optics (Ap-

[1] The documentation of TensorBoard can be found in https://www.tensorflow.org/tensorboard?hl=es-419

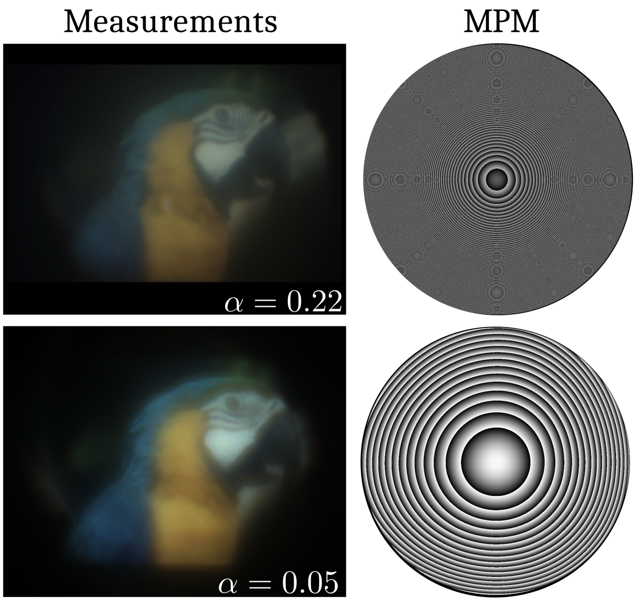

Fig. 3. Experimental blurred measurements produced by two different MPMs for $\alpha = 0.22$, 0.05, and Fresnel order equal to 1.4. These results reveal that the measurements produced by the MPM for $\alpha = 0.22$ is less bright at the sensor than the blurred data of the MPM for $\alpha = 0.05$. In fact, this physical effect is expected because larger α increases the phase aberration introduced by the MPM which means that light is more dispersed due to diffraction phenomenon.

pendix B in the paper). Then, we also present the behavior along epochs of the number of levels, the variable μ of the designed mixed OTF, and Tikhonov regularization parameter γ, in order to study their convergence. These results are summarized in Figs. 1 and 2.

We note from Fig. 1 that the proposed end-to-end design optimization has a convergence behavior since the loss function and the two verification quality imaging metrics smoothly start to achieve a maximum value after 100 epochs. Additionally, from Fig. 2 we observe that the number of levels, μ, and γ parameters also achieved a stable minimum value after 80 epochs. Since we are employing a smoothing function to optimize the number of levels, we can conclude the effectiveness of this function and joint optimization design.

2. COMPLEMENTARY EXPERIMENTAL RESULTS

A. Effects of Optical Power-sharing Variable α

We use $\alpha \in [0, 1]$ in order to share the quadratic phase delay between the lens and MPM. Fig. 3 shows how the changes of α from 0.22 to 0.05 influence the shape of MPM under SLM setup (in Section 5 of paper) and observed blurred image, with the Fresnel order equal to 1.4. Observe that these results reveal that the phase profile of the MPM is changed dramatically and the blurred data produced by the MPM for $\alpha = 0.22$ is less bright at the sensor than the blurred data of the MPM for $\alpha = 0.05$. In fact, this physical effect is expected because larger α increases the phase aberration introduced by the MPM which means that light is more dispersed due to diffraction phenomenon. Indeed, we recall that the optimal value for α found by our end-to-end optimization design is 0.05 for the setup exposed in Fig. 7 (of the paper).

B. Optimized Optical Power-Balanced Hybrid vs Lens + cubic phase MPM

In this section, we present blurred data and images reconstructed from the observed blurred measurements for two distances d_1 (0.5 and 1.0)m and two Fresnel orders (1.2 and 1.4) using the varying/invariant Wiener filtering methods as in Eq. (11) and Eq. (12) (of the paper), respectively. We also present the experimental PSFs for each system and different distances employing the process acquisition for the physical setup. This experimental data is acquired for the proposed optimized optical power-balance hybrid (with and without Zernike polynomials term), MPM corresponding to the cubic input phase, and lens systems with the intention of confirming the experimental results provided in Section 5 of the paper. We recall that the value for the optical power-sharing variable α is fixed as 0.05. The estimated images are obtained using the reconstruction algorithms (Section 3 in the paper). Note, that the OTF step in this algorithm demands the choice of the *reg* value following Eq. (11) and Eq. (12). In this section, we select *reg* by cross-validation to obtain the best visual quality for the reconstructed image in the interval $[10^{-5}, 10^{-3}]$.

From Fig. 4 we conclude that the highest value of Fresnel order and the varying Wiener filtering provides the best results in both image sharpening and low color aberrations for the proposed optical power-sharing hybrid. To see this, let us compare the image shown in column 'Fresnel order=1.4', row 'varying Wiener filter' versus all other results which are its counterparts. This image, which we call 'reference image' for $d_1 = 0.5$, is sharper than the reconstructed scene obtained with Fresnel order=1.2 (column 'Fresnel order=1.2', row 'varying Wiener filter') as shown from the insertions of the zoomed parts of these images. Comparing the reference image versus the other reconstructions in this row, we again see the advantage of this reconstruction in its sharpness. In addition, analyzing the reference image versus the reconstructions shown in the row 'Invariant Wiener filter', we note strong color aberrations in the zoomed insertions for these images which do not exist in the reference image. Moreover, taking now as the reference, image in column 'Fresnel order=1.4', row 'varying Wiener filter' for $d_1 = 1.0$ and comparing it with its counterparts in this distance, we conclude the advantage of the proposed optical power-balanced hybrid (with Zernike polynomials term) system in both stronger sharpness and decreased color aberrations.

3. CHROMATIC ANALYSIS OF OPTICAL POWER-BALANCED HYBRID SYSTEM

In Fig. 5 we present the results obtained using a color check palette as a scene in order to study the chromatic aberrations in the analyzed systems. From this scenario, using as the reference images for $d_1 = 0.5, 1.0$ (column Fresnel order=1.4, rows 'varying Wiener filter'), we confirm that the highest value of Fresnel order provides the highest reconstruction quality since the inserted zoomed images show strong chromatic aberrations for the rest of the images for each distance. For instance, in the zoomed images for the brown color, we see red lines which means a chromatic disorder introduced by the optics of the just lens, lensless with cubic phase MPM (column β), and hybrid lens+cubic phase MPM (column $\alpha + \beta$) systems. It is worth noticing that these chromatic distortions appear whether the color at the scene is bright or dark; which proves the effectiveness of the proposed system. Moreover, these results are aligned with the observations in Fig. 4 suggesting that the lens+cubic phase MPM, lensless cubic phase MPM, and lens systems pro-

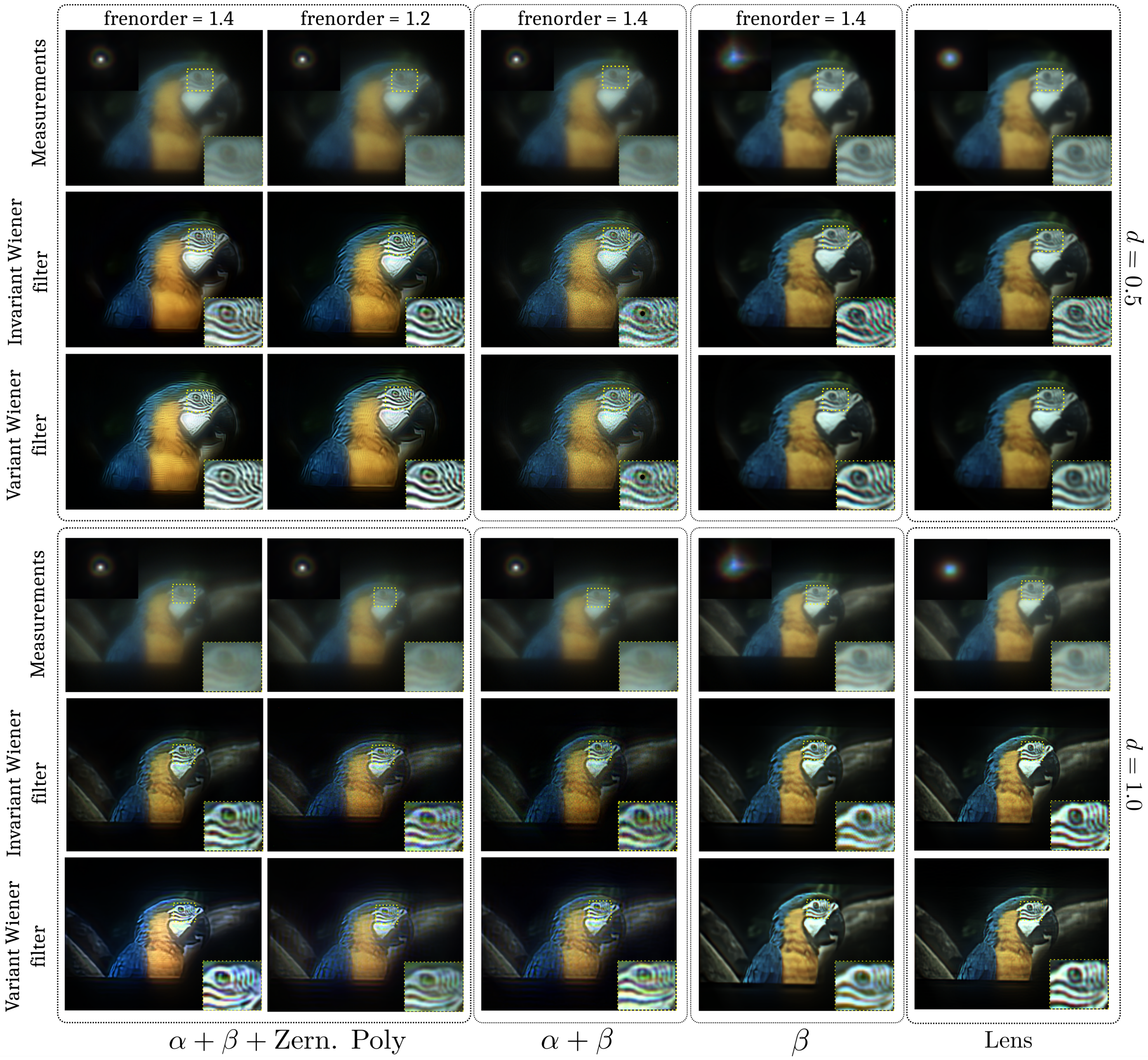

Fig. 4. Images reconstructed from experimental blurred observations ('Measurements' rows) using invariant/varying Wiener filtering OTFs at two distances ($d_1 = 0.5, 1.0$), and two Fresnel order for the compared optical setups: the proposed optical power-balanced hybrid (column $\alpha + \beta +$ Zernike polynomial), optical power-balanced hybrid with exclusion of the third term (column $\alpha + \beta$), lensless with a MPM corresponding to cubic companion (column β), and lens only (column Lens). We also show, in the measurements rows (left corners of the images), the experimental PSFs for all compared systems. These results suggest that the highest value of Fresnel order provides the best quality reconstructions and that the advantage of the varying Wiener filtering OTFs in Eq. (11) over its invariant version in Eq. (12) is in mitigation of the chromatic aberrations and reduction of the noise. Additionally, we notice that the optimized proposed optical power-balance hybrid system is superior to its lens + cubic phase MPM (column $\alpha + \beta$), lensless with cubic MPM (column β), and lens competitors in terms of sharpness and chromatic aberrations suggesting the effectiveness of the optimization framework.

vide strong chromatic aberrations in the reconstructed images. In fact, it is now clearer that the advantage of the varying Wiener filtering over its invariant version is the mitigation of the chromatic aberrations and reduction of the noise. Thus, we have that the optimization framework indeed provides phase-coded optics for desired improved achromatic extended-depth-of-field imaging.

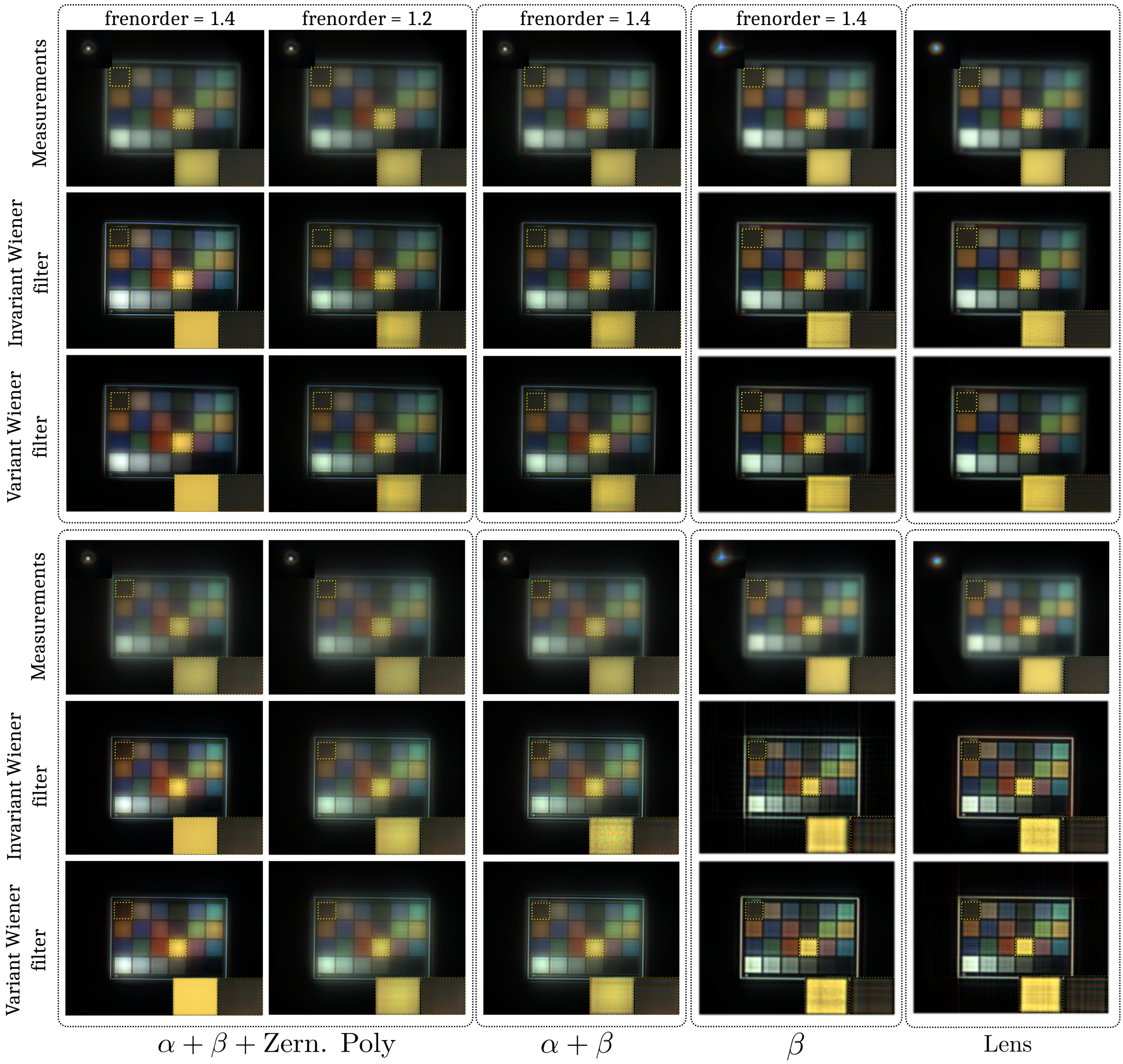

Fig. 5. Images reconstructed from experimental blurred observations ('Measurements' rows) using invariant/varying Wiener filtering at two distances ($d_1 = 0.5, 1.0$), and two Fresnel order for the compared optical setups: the proposed optical power-balanced hybrid (column $\alpha + \beta + 14$ poly), optical power-balanced hybrid with exclusion of the third term (column $\alpha + \beta$), lensless with a MPM corresponding to cubic companion (column β), and lens only (column Lens). We also show, in the measurements rows (left corners of the images), the experimental PSFs for all compared systems. This experiment is intended to study the chromatic behavior of the proposed system. In fact, these results confirm that the highest value of Fresnel order provides the best reconstruction quality and that the advantage of the varying Wiener filtering over its invariant version is a mitigation of the chromatic aberrations and reduction of the noise. Additionally, we verify that the optimized proposed optical power-balance hybrid system is superior to its lens + cubic phase MPM (column $\alpha + \beta$), lensless with cubic MPM (column β), and lens competitors in terms of sharpness and chromatic aberrations suggesting the effectiveness of the optimization framework.